Fluorescent probes based on acridine derivatives and their application in dynamic monitoring of cell polarity variation

Hai-Yan Peng,[a] Gang Zhang,[b] Ru Sun,[*,a] Yu-Jie Xu,[b] Jian-Feng Ge[*,a]

[a] *College of Chemistry, Chemical Engineering and Material Science, Soochow University, 199 Ren'Ai Road, Suzhou 215123, China.*

[b] *State Key Laboratory of Radiation Medicine and Protection, School of Radiation Medicine and Protection and Collaborative Innovation Center of Radiation Medicine of Jiangsu Higher Education Institutions, Soochow University, Suzhou 215123, China.*

Index

* *Corresponding authors. E-mail addresses: sunru924@hotmail.com (R. Sun), ge_jianfeng@hotmail.com (J.-F. Ge).*

Table S1. Optical properties of probe **1a** in different solvents.

Probe	Solvents	Δf	$\lambda_{Abs,max}$[a]	$\lambda_{Em,max}$[a]	Stokes shift[a]	ε[b]	Φ[c]
1a	H_2O	0.3200	355	594	239	2.47	0.50
1a	DMSO	0.2640	351	583	232	3.34	3.06
1a	MeCN	0.3040	345	580	235	3.26	3.43
1a	MeOH	0.3092	345	574	229	3.88	3.83
1a	EtOH	0.2887	345	570	225	4.46	5.24
1a	DCM	0.2170	346	560	214	3.85	5.57
1a	THF	0.2086	347	562	215	3.57	5.82
1a	EA	0.1990	346	560	214	3.39	8.00
1a	Dioxane	0.0205	348	565	217	3.60	11.1
1a	TOL	0.0153	348	553	205	3.68	35.6

Table. S2. Optical properties of probe **1b** in different solvents.

Probe	Solvents	Δf	$\lambda_{Abs,max}$[a]	$\lambda_{Em,max}$[a]	Stokes shift[a]	ε[b]	Φ[c]
1b	H_2O	0.3200	364	572[d]	208	1.00	0.51
1b	DMSO	0.2640	366	568[d]	202	1.02	0.63
1b	MeCN	0.3040	366	557	191	0.98	1.42
1b	MeOH	0.3092	366	555	189	0.96	1.32
1b	EtOH	0.2887	366	556	190	0.87	1.47
1b	DCM	0.2170	367	548	181	1.04	2.18
1b	THF	0.2086	366	541	175	1.12	3.58
1b	EA	0.1990	364	535	171	1.06	9.93
1b	Dioxane	0.0205	364	535	171	1.24	13.5
1b	TOL	0.0153	366	534	168	0.97	13.2

Table. S3. Optical properties of probes **1c-d** in H_2O and glycerol.

Probe	Solvents	$\lambda_{Abs,max}$[a]	$\lambda_{Em,max}$[a]	Stokes shift[a]	ε[b]	Φ[c]
1c	H_2O	366	442	76	1.65	0.30
1c	Glycerol	362	445	83	0.93	12.48
1d	H_2O	362	538	176	0.70	0.12
1d	Glycerol	365	532	167	0.98	9.20

[a] Reported in nm.

[b] Reported in 10^4 M^{-1} cm^{-1}.

[c] Reported in %. Coumarin–153 (Φ=0.544 in ethanol) was used as the reference compound in test.

[d] Second highest peak.

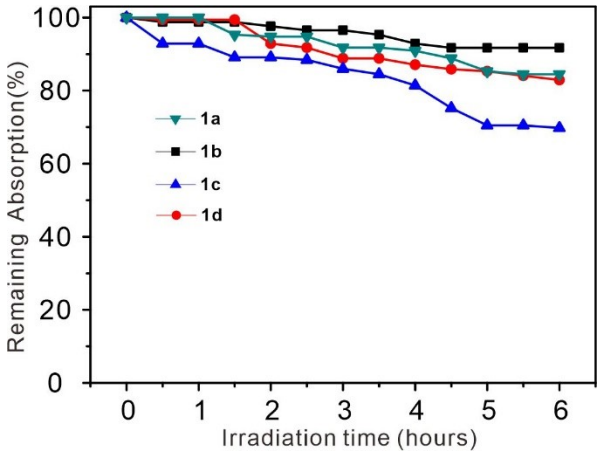

Fig. S1. Photofading behaviors of probes **1a-d** in acetonitrile.

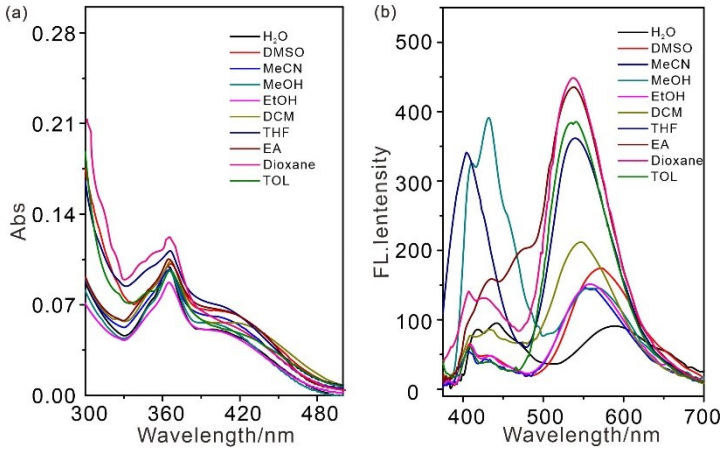

Fig. S2. Optical properties of probe **1b** (10 μM) in different solvents. (a) Absorption spectra; (b) emission spectra (excited at 362 nm, slit widths: 5 nm/10 nm).

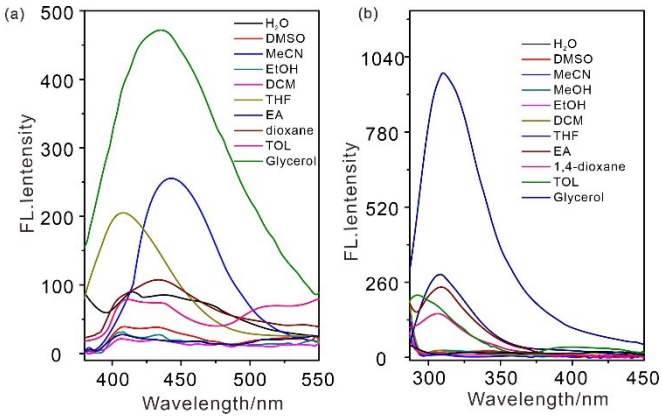

Fig. S3. Emission spectra of probes **1c-d** in different solvents. (a) emission spectra of **1c**; (b) emission spectra of **1d.**

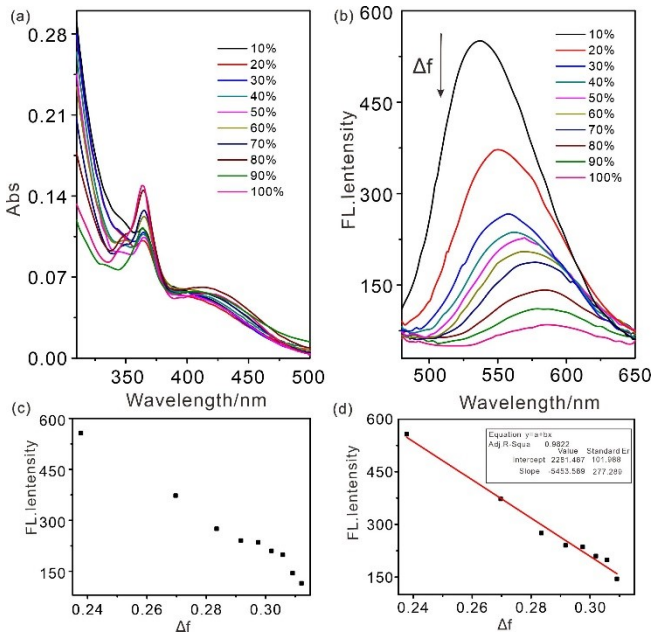

Fig. S4. Optical responses of probe **1b** (10 μM) in dioxane/H_2O mixtures with increasing polarity (water from 10% to 100%). (a)Absorption spectra; (b)emission spectra (λ_{ex}=362 nm, slit widths: 5 nm/10 nm); (c) relationship between fluorescence intensity (570 nm) and Δ*f*; (d) linear relationship of fluorescence intensity at 570 nm versus Δ*f* (0.238–0.315).

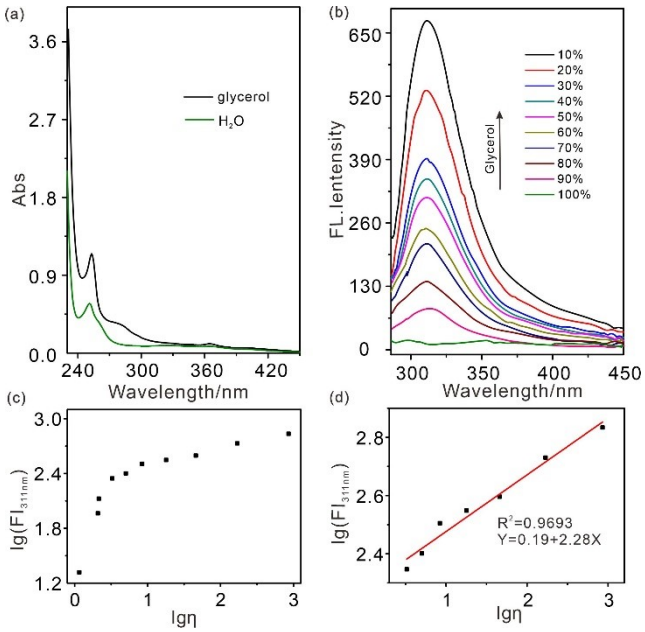

Fig. S5. Optical responses of probe **1d** (10 μM) in glycerol/H_2O mixtures with increasing viscosity (water from 100% to 1%). (a)Absorption spectra; (b)emission spectra (λ_{ex}=282 nm, slit widths: 5 nm/10 nm); (c)relationship between lg(I_{311nm}) and lgη; (d)linear relationship of lg(I_{311nm}) versus lgη.

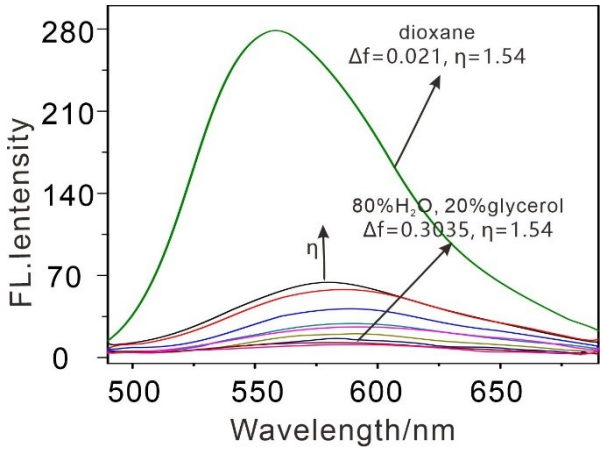

Fig. S6. The fluorescence spectra of probe **1a** (10 μM) in H_2O/glycerol mixture under different viscosity.

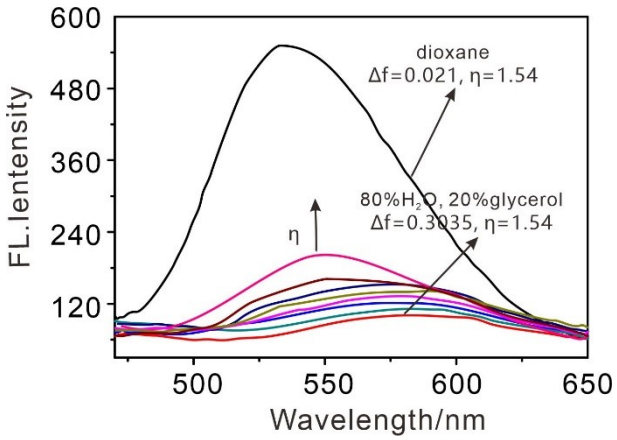

Fig. S7. The fluorescence spectra of probe **1b** (10 μM) in H_2O/glycerol mixture under different viscosity.

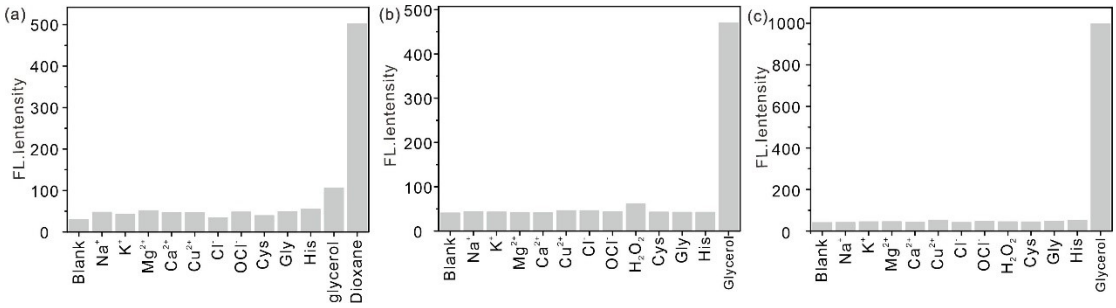

Fig. S8. Selectivity experiments of probes **1b-d** (10 μM) toward different analytes. 5 mM for Ca^{2+}, Mg^{2+}, Cu^{2+}, Cl^-, OCl^-, H_2O_2; 10 mM for K^+, Na^+, Cys, Gly, His. (a)probe **1b** (λ_{ex}=362 nm, slit widths: 5 nm/10 nm). (b)probe **1c** (λ_{ex}=360 nm, slit widths: 5 nm/10 nm). (c)probe **1d** (λ_{ex}=282 nm, slit widths: 5 nm/10 nm).

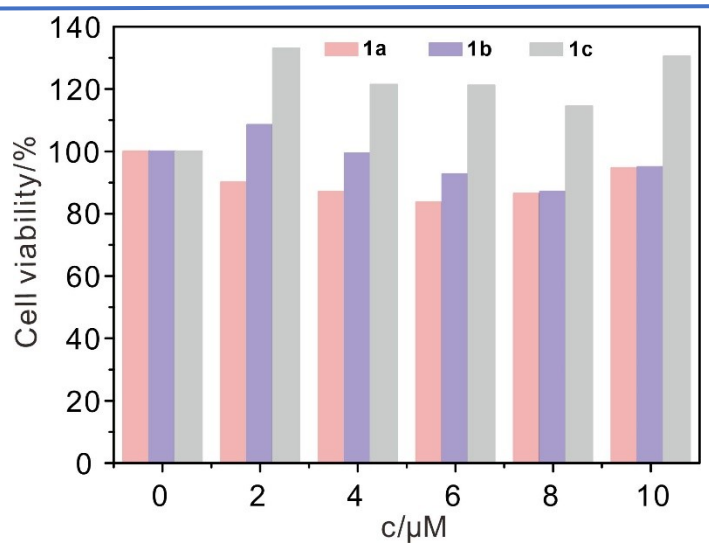

Fig. S9. HeLa cells viabilities after treatment with probes **1a-c**. Cell viability was assayed by the CCK-8 method.

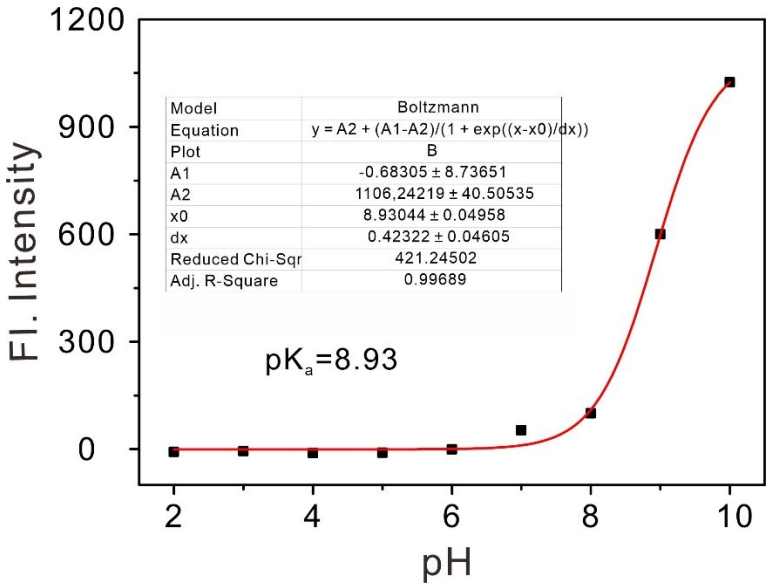

Fig. S10. Fluorescence intensity of probe **1b** at different pH.

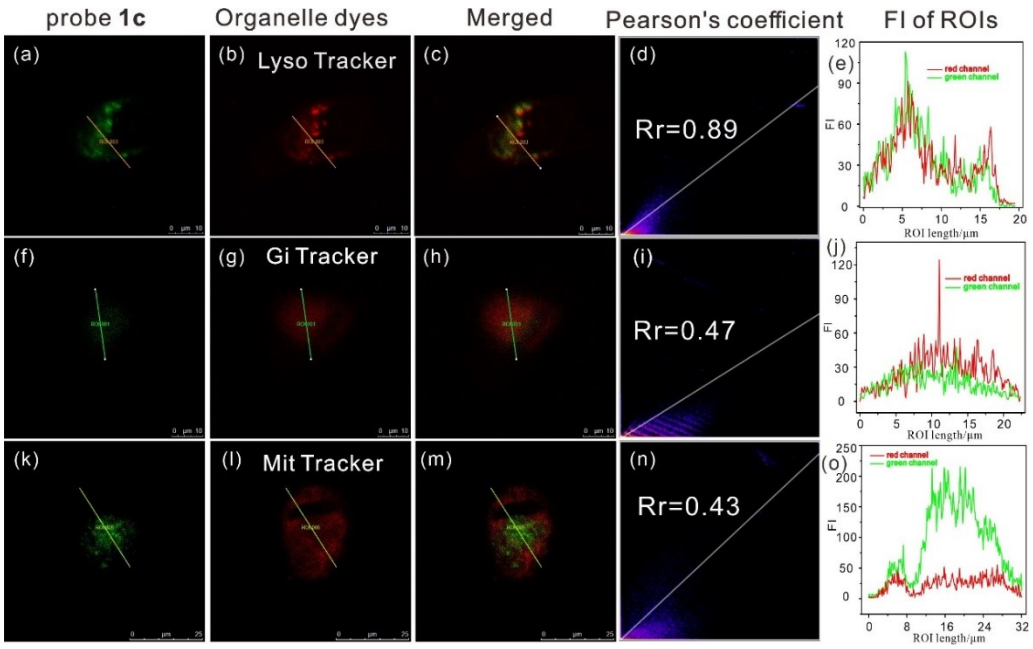

Fig. S11. Fluorescence confocal images of living HeLa cells with probe **1c** and ROI analysis: (a, f, k) confocal image (green channel) of cells with probe **1c** (6 μM); (b, g, l) confocal image (red channel) of cells with Lyso-Tracker Red DND-99 (100 nM), Gi-Tracker Red (100 nM) or Mito-Tracker®Red CMXRos (100 nM); (c, h, m) merged image of the green and red channels; (d, i, n) fluorescence intensity correlation plot of the green and red channels; (e, j, o) fluorescence intensities of the regions of interest (ROIs) across the cells.

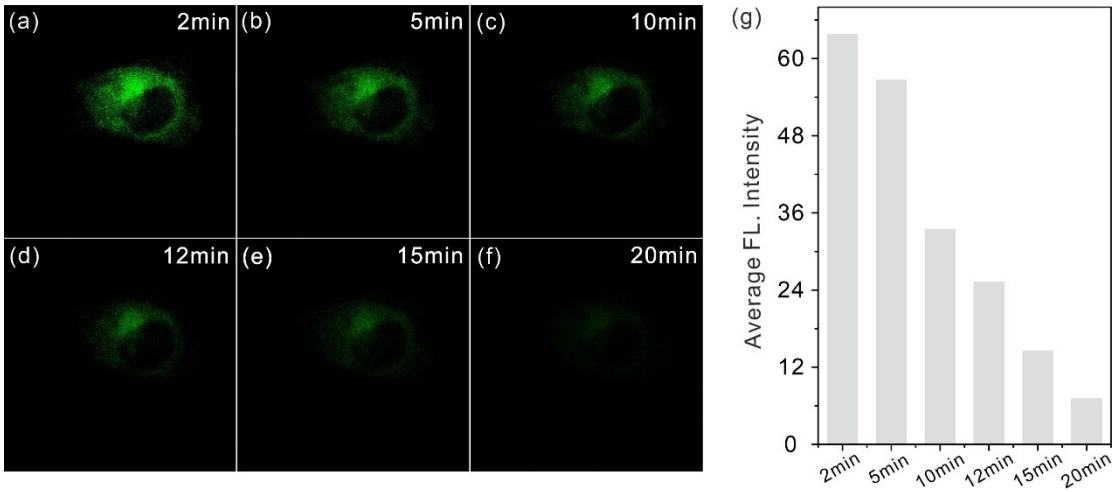

Fig. S12. Photobleaching experiment of probe **1c**. (a-f) The cell image of probe **1c** after laser irradiation for different times in HeLa cells. (g) average fluorescence intensity of green channel after irradiation for different times.

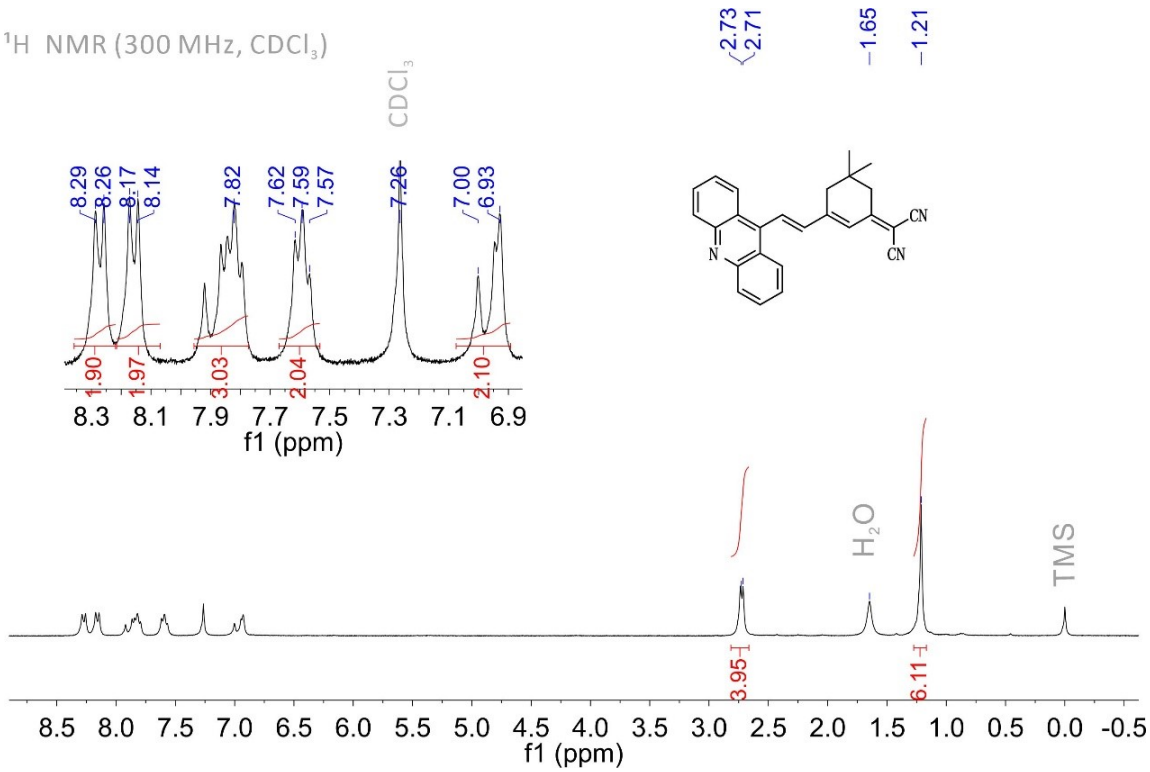

Fig. S13. ^{1}H NMR spectrum of probe **1a**

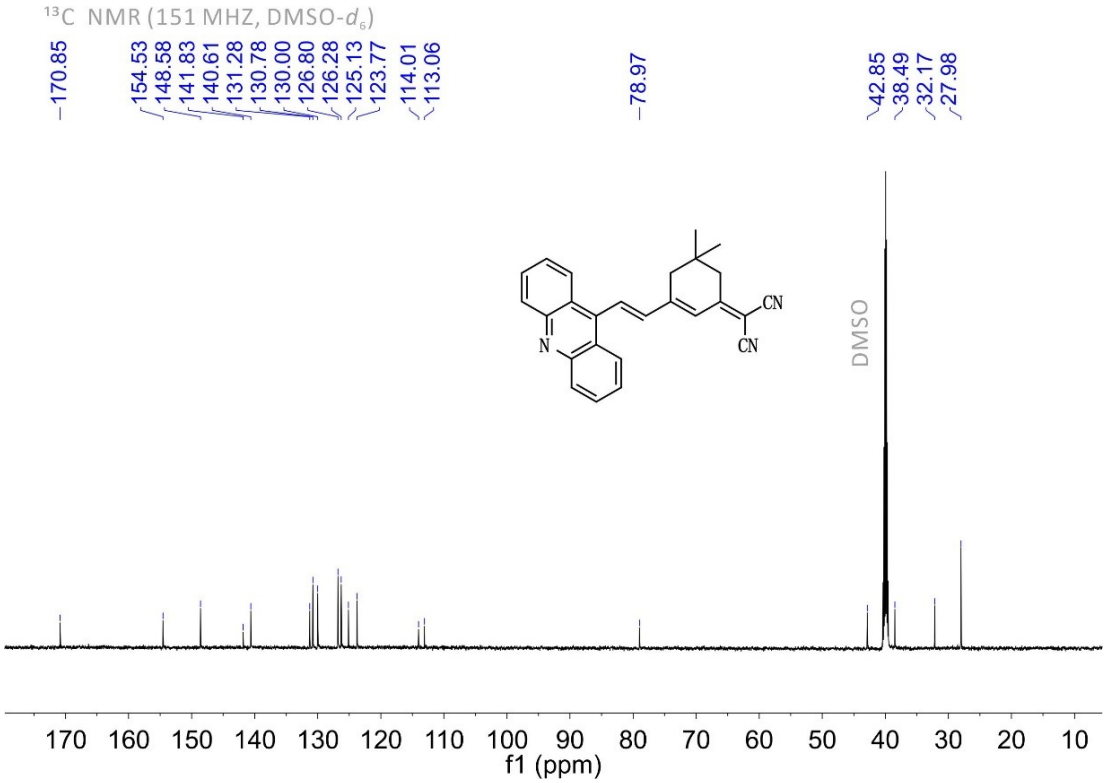

Fig. S14. ^{13}C NMR spectrum of probe **1a**

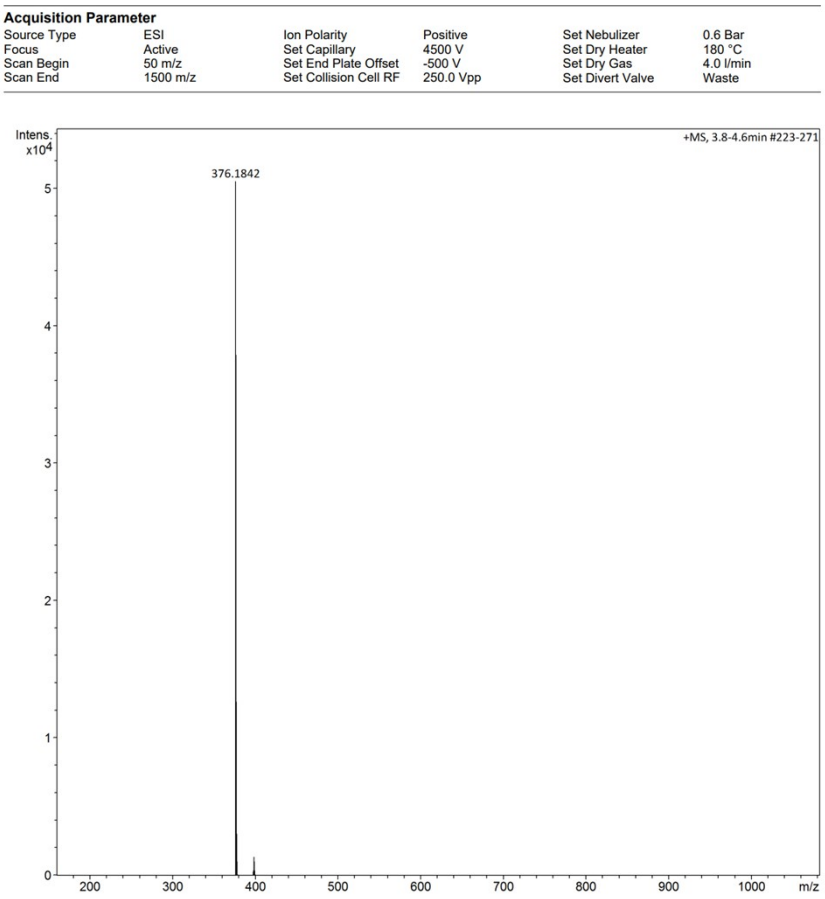

Fig. S15. HRMS(ESI⁺) spectrum of probe **1a**

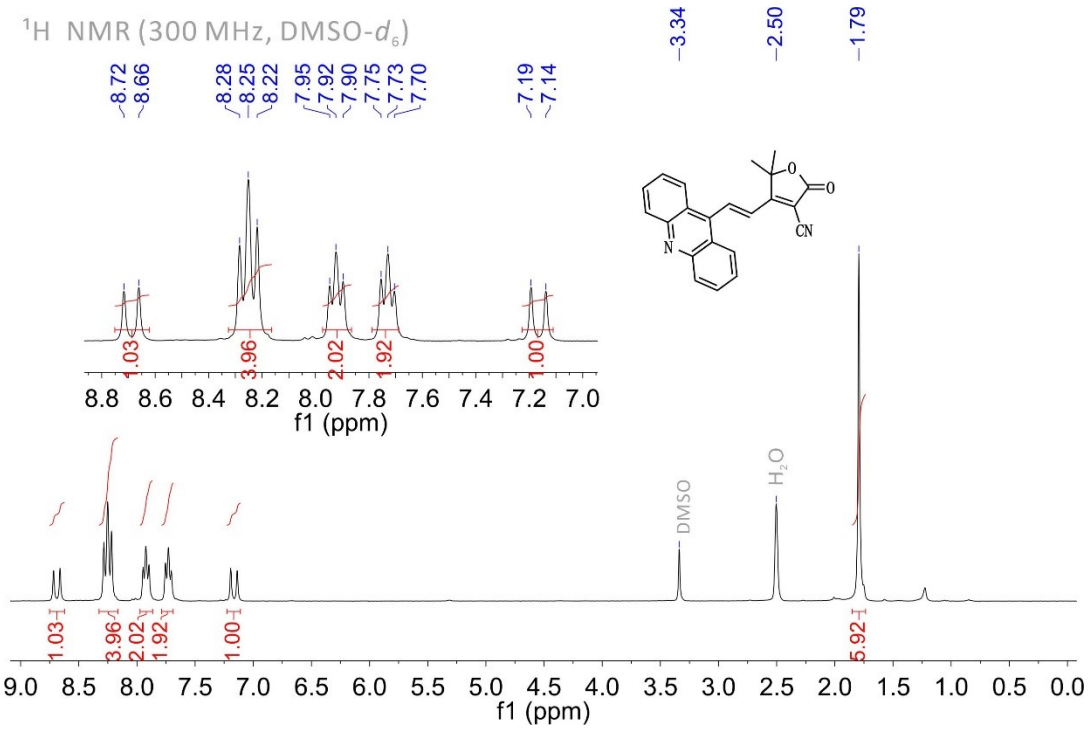

Fig. S16 ¹H NMR spectrum of probe **1b**

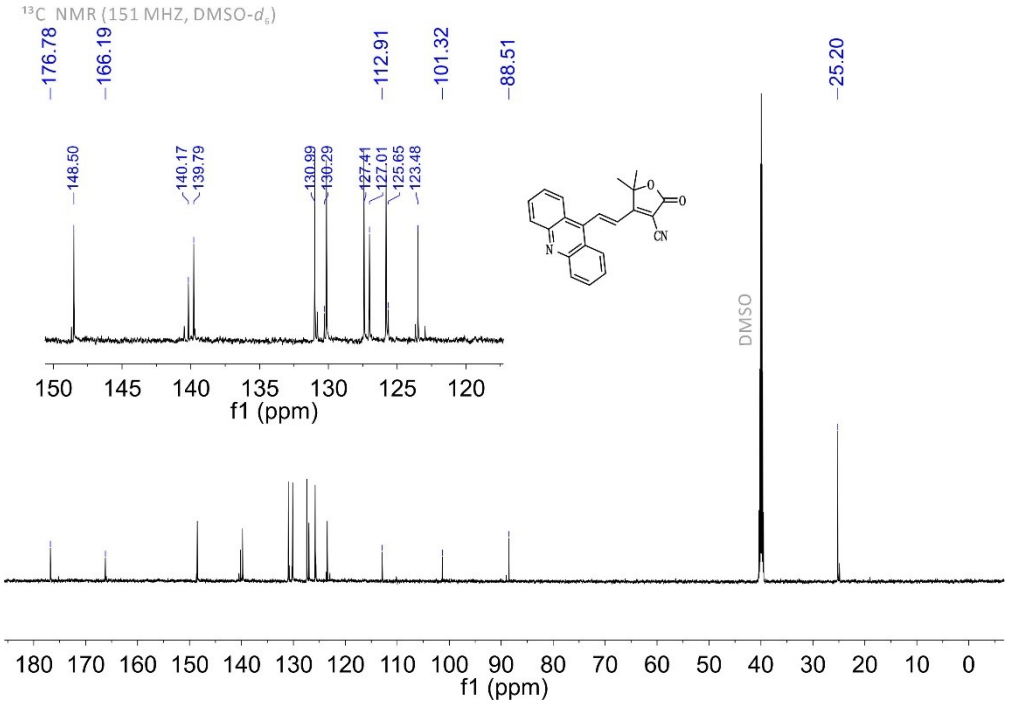

Fig. S17 ^{13}C NMR spectrum of probe **1b**

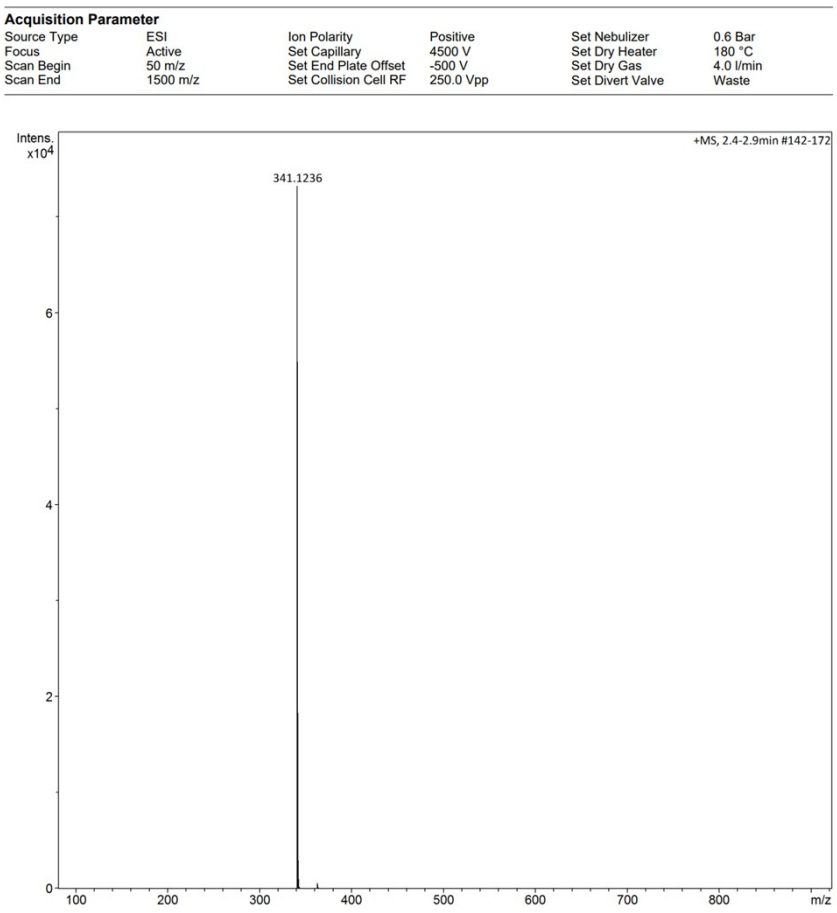

Fig. S18 HRMS(ESI$^+$) spectrum of probe **1b**

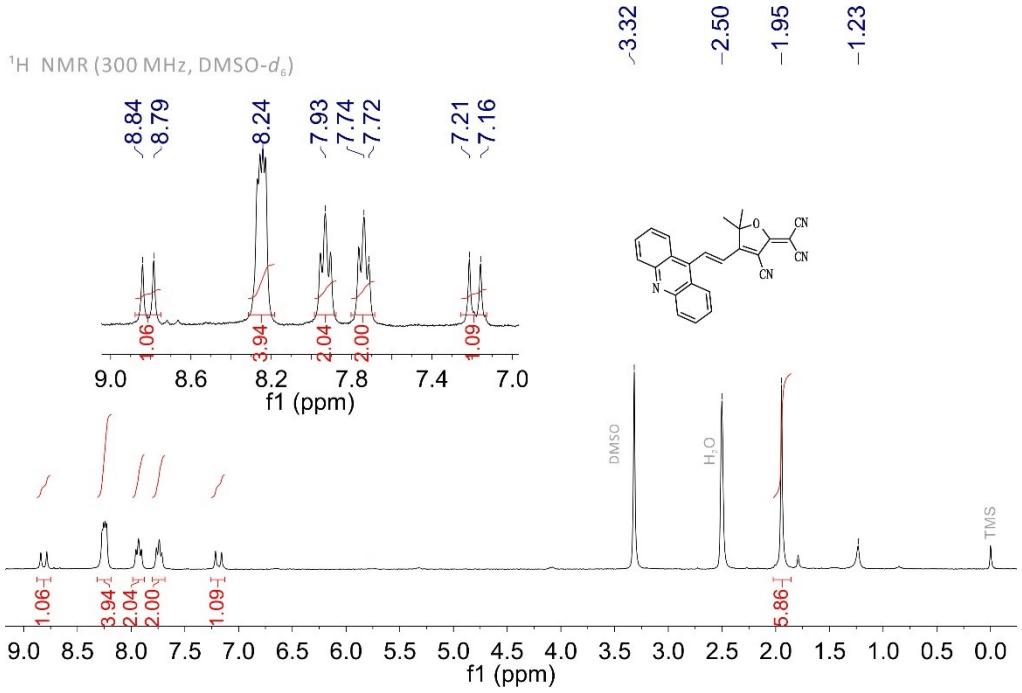

Fig. S19 ^{1}H NMR spectrum of probe **1c**

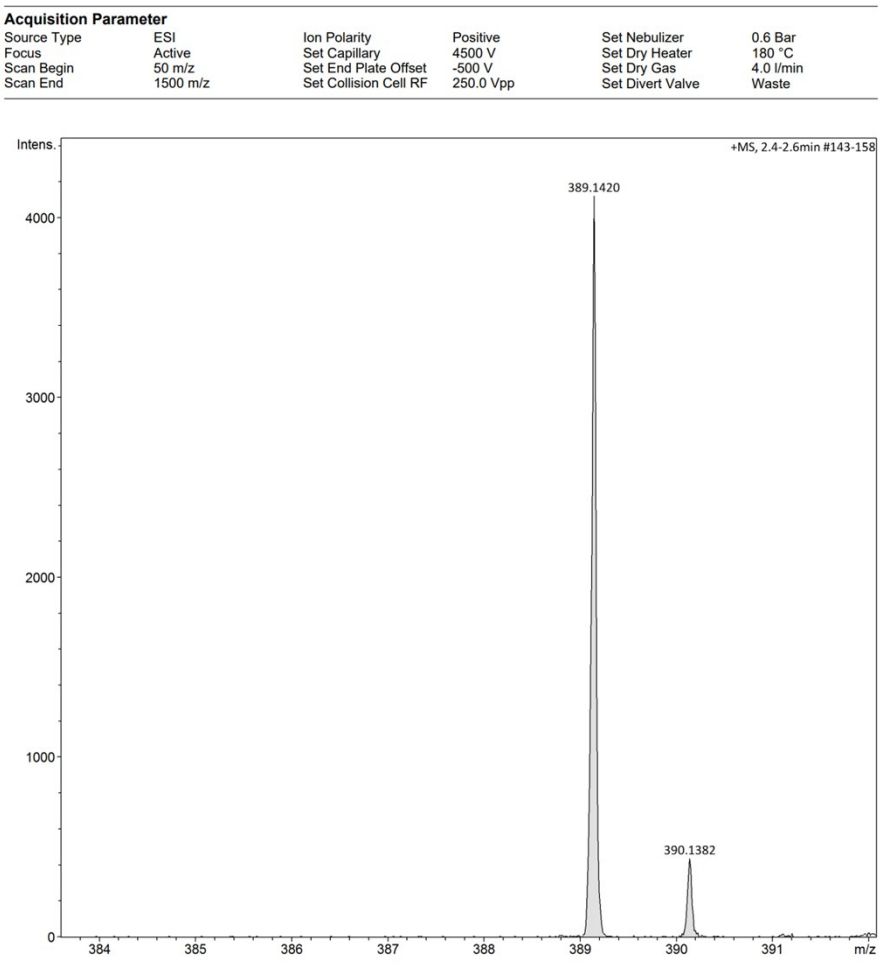

Fig. S20 HRMS(ESI^{+}) spectrum of probe **1c**

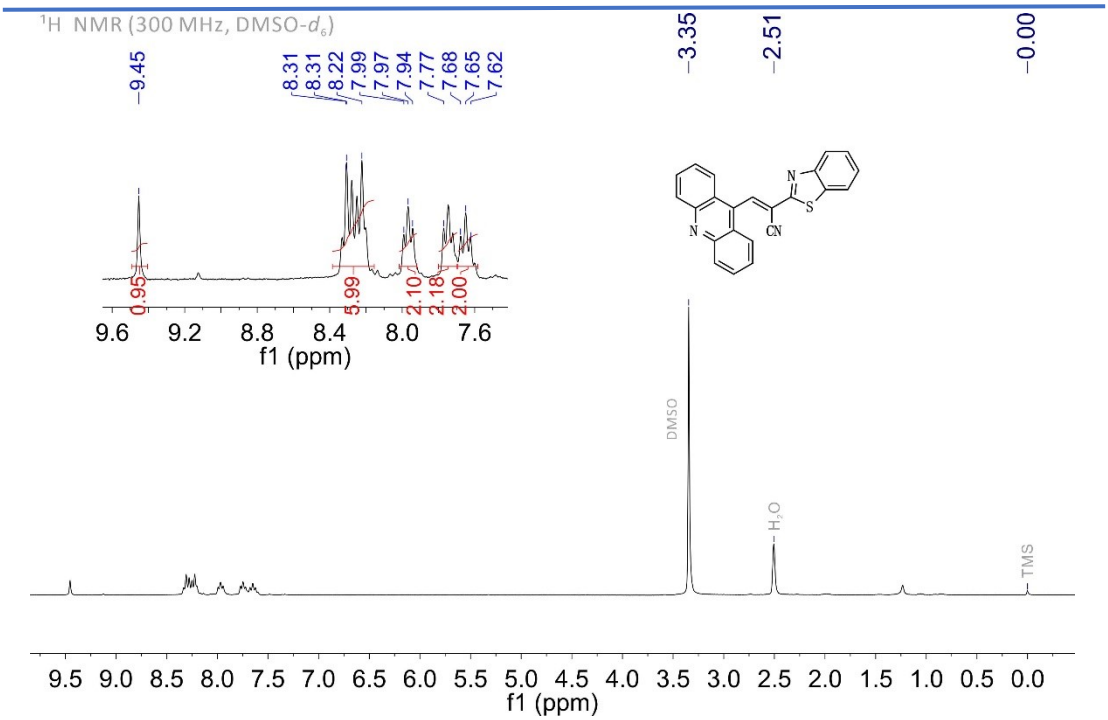

Fig. S21 ^{1}H NMR spectrum of probe **1d**

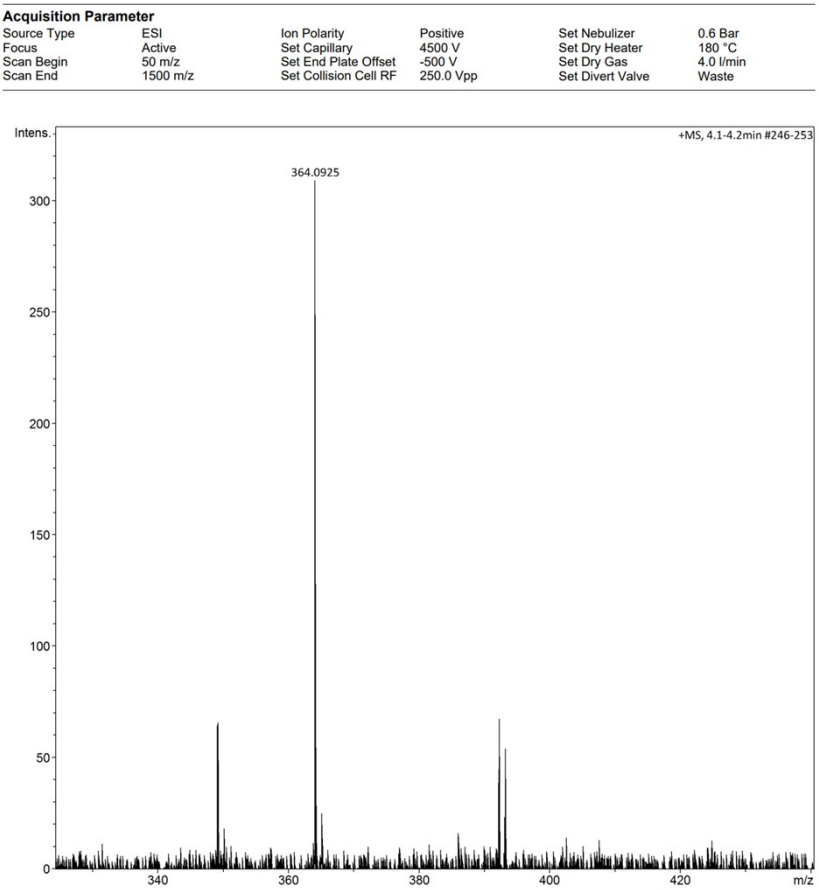

Fig. S22. HRMS(ESI^{+}) spectrum of probe **1d**